# Phase-field simulation of the microstructure evolution in the eutectic NiAl-34Cr system

Michael Kellner [a,*], Ioannis Sprenger [c], Philipp Steinmetz [a], Johannes Hötzer [a,b], Britta Nestler [a,b], Martin Heilmaier [c]

[a] Institute for Applied Materials - Computational Materials Science (IAM-CMS), Karlsruhe Institute of Technology (KIT), Haid-und-Neu-Str. 7, 76131 Karlsruhe, Germany
[b] Institute of Materials and Processes, Karlsruhe University of Applied Sciences, Moltkestrasse 30, D 76133 Karlsruhe, Germany
[c] Institute for Applied Materials - Institute of Materials Science and Engineering (IAM-WK), Karlsruhe Institute of Technology (KIT), Kaiserstr. 12, 76131 Karlsruhe, Germany

## ARTICLE INFO

## ABSTRACT

The directionally solidified eutectic alloy NiAl-34Cr possesses promising properties for structural applications at high temperatures, such as increased creep resistance compared to the stoichiometric NiAl, while keeping the excellent oxidation behavior of the binary intermetallic compound. As microstructure and material properties are usually closely linked together, a deeper understanding of the microstructure evolution is crucial to design materials with defined properties. To simulate the eutectic reaction during directional solidification (DS), a thermodynamically consistent phase-field model based on the Grand potential approach is applied. Two- and three-dimensional simulations of the DS process for three different growth velocities are performed. The evolving microstructures obtained from large-scale simulations are presented and compared with micrographs from scanning electron microscopy (SEM) as well as with the analytic Jackson-Hunt approach in 2D and 3D. The simulation results are in qualitative and quantitative accordance with both, DS experiments and analytical solutions.

© 2016 Elsevier B.V. All rights reserved.

## 1. Introduction

The intermetallic compound NiAl, with its high melting point ($T_m = 1911$ K), low density (5.95 g/cm$^3$), high thermal conductivity ($> 70$ W/K m) and excellent oxidation resistance is of particular interest for technical applications at elevated temperatures such as turbine blades in jet engines or stationary gas turbines [1,2]. Apart from these advantages, NiAl possesses a low fracture toughness and ductility at room temperatures as well as an insufficient strength at high temperatures and a poor creep resistance [3]. One potential way to overcome those disadvantages is to introduce a second reinforcing phase by the addition of refractory metals (e.g. Cr, Mo and W) [4] and subsequent directional solidification of quasi-binary eutectics made thereof. For example the ternary system Ni-Al-Cr contains a binary eutectic reaction at 34 at.%Cr, 33 at.% Ni and 33 at.%Al between the liquid and the two solid phases NiAl (ordered B2) and Cr (disordered A2) [5,6]. During directional solidification, Cr–rich fibers grow parallel to the NiAl–Matrix with a strong crystallographic relationship $(100)_{NiAl}||(100)_{Cr}$ [7]. The fiber diameter and spacing can be influenced by applied process parameters and conditions such as growth rate $v$ and temperature gradient $G$.

A SEM-micrograph parallel to the growth front of the DS eutectic NiAl-34Cr with a growth rate of 80 mm/h is depicted in Fig. 1 and exemplary shows a typical microstructure of the binary two-phase eutectic. The micrograph contains the Cr fibers as bright phase with an area fraction of $36 \pm 3\%$ embedded in a dark NiAl matrix. To investigate the evolution of directionally solidified microstructures phase-field simulations have been established in the recent years. The phase-field method allows to simulate different physical effects at various micro- and macroscopic scales for several magnitudes of temperature [8].

The results endow insight into the microstructure evolution in three-dimensions and predict the microstructure responses depending on the variation of the physical parameters, in addition to the two-dimensional sections of experimental micrographs. Simulations of a hexagonal arrangement of rods embedded in a continuous matrix for a binary system are reported by Parisi and Plapp [9]. The growth of two solid phases in ternary systems with impurities, forming eutectic colonies, are studied by large-scale phase-field simulations in [10–13]. Phase-field studies of the
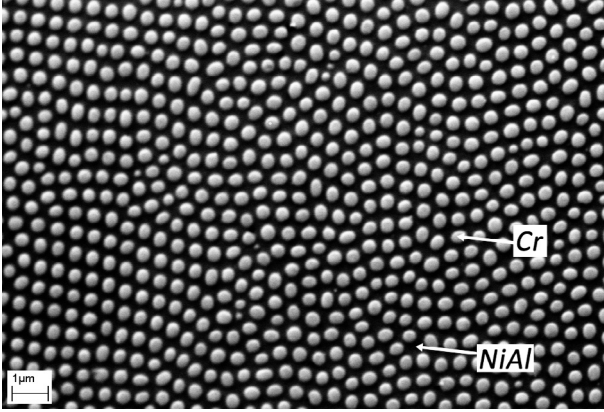
**Fig. 1.** Transversal section of the microstructure of the directionally solidified NiAl-34Cr showing typical arrangement of Cr-fibers.

system Ni-Al-Cr have been conducted to investigate the mechanical properties in [14,15] as well as diffusion paths in [16,17].

The focus of this work is the validation of a simulation model for NiAl-34Cr by experimental and analytic solutions in order to predict the microstructure evolution during directional solidification at different growth velocities. First the experimental setup is introduced. Then, the applied phase-field model, the mathematical approaches to obtain the physical parameters are described and an introduction of the Jackson-Hunt analysis is given. Afterwards, the simulation setup is shown and the used physical as well as numerical parameters are explained. For the validation of the model and the parameters, two- and three-dimensional simulations for different arrangements of the rods are compared with the analytical Jackson–Hunt approach [18]. Following, large-scale 3D phase-field calculations are comparatively assessed with experimental results for 20 mm/h, 50 mm/h and 80 mm/h and subsequently the conclusions are drawn.

## 2. Methods

### 2.1. Experimental setup

The alloy with the nominal composition of NiAl-34Cr is synthesized from Ni, Al, and Cr high purity elements ($> 99.99\%$ pure) with an arc-melter under protective argon atmosphere. Three buttons with a mass of 250 g each are produced in a first step and remelted 5–7 times to achieve a sufficient homogeneity - the mass loss was in all cases below 0.2%. Thereafter, each button is cast into a cylindrical shaped copper crucible with a diameter of 12.5 mm and a length of 120 mm. In the final step the rods are directionally solidified (DS) in an optical floating zone furnace as described by Bei and George [19]. For the DS-process, constant growth rates of 20 mm/h, 50 mm/h and 80 mm/h are chosen and a constant counter clockwise rotation of 60 rpm is applied. The metallographic preparation comprises of grinding with subsequent polishing and etching in solution of 10% HCl and 10% $H_2O_2$ and 80% $H_2O$ (volume percent). The micrographs are acquired in a scanning electron microscope (SEM; Zeiss EVO 50, Oberkochen, Germany). For quantitative analysis of the microstructure, digital image software "Fiji" [20,21] is applied to obtain fiber diameter and spacing as well as area fractions of the phases. The diameter of each individual fiber is derived from its measured area using the equivalent circle diameter. In "Fiji" software this is accomplished by using the routine "particle analysis". To calculate the distance $\lambda$ between the rods, first the barycenter of each rod is determined. Subsequently a Delaunay triangulation is applied, which yields the nearest

neighbor distances between the barycenters of the adjacent fibers. In order to evaluate possible chemical deviations due to the processing, an energy-dispersive spectroscope (EDS; Thermo Fisher Model 226A-1SES, Waltham, MA) is used to measure the composition after the DS-step. The difference between the nominal and the actual composition is below of 1 at.% for each element.

### 2.2. Phase-field model

The phase-field model is composed on the basis of the Grand potential approach [22,23] in a thermodynamic consistent way. The implementation of the model is presented in [24–26] and further applications of the model for DS are reported in [24,27–29]. The chemical potential $\mu_\alpha^i$ of a component $i \in \{1 \dots K\}$ for the phase $\alpha \in \{1 \dots N\}$ is defined as

$$\mu_\alpha^i(\mathbf{c}) = \frac{\partial f_\alpha(\mathbf{c}, T)}{\partial c_\alpha^i},$$ (1)

derived from the free energy $f_\alpha(\mathbf{c}, T)$. Different chemical potentials for coexisting phases result in a diffusion process, which lead to an adjustment of the potentials. Therefore,

$$\underbrace{\frac{1}{\epsilon}T\frac{\partial \omega(\phi)}{\partial \phi_\alpha} - \sum_{\beta=1}^{N} \psi_\beta(\boldsymbol{\mu}, T)\frac{\partial h_\beta(\phi)}{\partial \phi_\alpha}}_{:=rhs_{\beta 2}}$$

the chemical potentials can be reduced to

$$\boldsymbol{\mu} = \begin{pmatrix} \mu^1 \\ \mu^2 \\ \vdots \\ \mu^K \end{pmatrix} = \begin{pmatrix} \mu_\alpha^1 \\ \mu_\alpha^2 \\ \vdots \\ \mu_\alpha^K \end{pmatrix} = \begin{pmatrix} \mu_\beta^1 \\ \mu_\beta^2 \\ \vdots \\ \mu_\beta^K \end{pmatrix} = \dots = \begin{pmatrix} \mu_N^1 \\ \mu_N^2 \\ \vdots \\ \mu_N^K \end{pmatrix}$$ (2)

[22,30]. The following coupled time evolution equations $\partial \cdot /\partial t$ are derived for $N$ phase-fields $\phi_\alpha$, based on an Allen–Cahn approach, for $K$ chemical potentials $\boldsymbol{\mu}$, based on the assumption of mass conservation as well as the temperature $T$:

$$\tau\epsilon\frac{\partial \phi_\alpha}{\partial t} = \underbrace{-\epsilon T\left(\frac{\partial a(\phi, \nabla\phi)}{\partial \phi_\alpha} - \nabla \cdot \frac{\partial a(\phi, \nabla\phi)}{\partial \nabla\phi_\alpha}\right)}_{:=rhs_{\beta 1}}$$

$$\underbrace{-\frac{1}{\epsilon}T\frac{\partial \omega(\phi)}{\partial \phi_\alpha} - \sum_{\beta=1}^{N} \psi_\beta(\boldsymbol{\mu}, T)\frac{\partial h_\beta(\phi)}{\partial \phi_\alpha}}_{:=rhs_{\beta 2}}$$

$$-\frac{1}{N}\sum_{\beta=1}^{N}(rhs_{\beta 1} - rhs_{\beta 2}),$$ (3)

$$\frac{\partial \boldsymbol{\mu}}{t} = \left[\sum_{\alpha=1}^{N} h_\alpha(\phi)\left(\frac{\partial \mathbf{c}_\alpha(\boldsymbol{\mu}, T)}{\partial \boldsymbol{\mu}}\right)\right]^{-1}\left(\nabla(\mathbf{M}(\phi, \boldsymbol{\mu}, T)\nabla\boldsymbol{\mu} - \mathbf{J}_{at}(\phi, \boldsymbol{\mu}, T))\right.$$

$$\left. - \sum_{\alpha=1}^{N} \mathbf{c}_\alpha(\boldsymbol{\mu}, T)\frac{\partial h_\alpha(\phi)}{\partial t} - \sum_{\alpha=1}^{N} h_\alpha(\phi)\left(\frac{\partial \mathbf{c}_\alpha(\boldsymbol{\mu}, T)}{\partial T}\right)\frac{\partial T}{\partial t}\right),$$ (4)

$$\frac{\partial T}{\partial t} = \frac{\partial}{\partial t}(T_0 + G(z - v\,t)) = -G\,v.$$ (5)

The parameter $\tau$ describes the kinetics of the interfaces and $\epsilon$ is related to its thickness. The form of the interface is modeled by the gradient energy density $a$ and the potential energy $\omega$. The driving force for the phase transitions is related to the phase dependent Grand potential $\psi_\beta$.

The functions $h_\beta$ define an interpolation between the different phases [31]. The term $\frac{1}{N}\sum_{\beta=1}^{N} rhs_\beta$ is a Lagrange multiplier accounting for the constraint $\sum_{\alpha=1}^{N} \partial\phi_\alpha/\partial t = 0$. The anti-trapping current $\mathbf{J}_{at}$